Parameter Scaling for the Fibonacci Point

LeRoy Wenstrom
Mathematics Department
S.U.N.Y. Stony Brook

Abstract

We prove geometric and scaling results for the real Fibonacci parameter value in the quadratic family $z \mapsto z^2 + c$. The principal nest of the Yoccoz parapuzzle pieces has rescaled asymptotic geometry equal to the filled-in Julia set of $z \mapsto z^2 - 1$. The modulus of two such successive parapuzzle pieces increases at a linear rate. Finally, we prove a "hairiness" theorem for the Mandelbrot set at the Fibonacci point when rescaling at this rate.

In this paper, we focus on the small scale similarities between the dynamical space and parameter space for the Fibonacci point in the family of maps $z \mapsto z^2 + c$. There is a general philosophy in complex dynamics that the structure we see in the parameter space around the parameter value c should be the "same" as that around the critical value 'c' in dynamical space [DH85]. In the case where the critical point is pre-periodic, Tan Lei [Lei90] proved such asymptotic similarities by showing that the Mandelbrot set and Julia set exhibit the same limiting geometry. For parameters in which the critical point is recurrent (i.e., it eventually returns back to any neighborhood of itself), the Mandelbrot and Julia sets are much more complicated. Milnor, in [Mil89], made a number of conjectures (as well as pictures!) for the case of infinitely renormalizable points of bounded type. Dilating by factors determined by the renormalization, the resulting computer pictures demonstrate a kind of self-similarity, with each successive picture looking like a "hairier" copy of the previous. McMullen [McM94] has proven that, for these points, the Julia set densely fills the plane upon repeated rescaling, i.e., hairiness; and Lyubich has recently proven hairiness of the Mandelbrot set for Feigenbaum like points. We focus on a primary example of dynamics in which we have a recurrent critical point and the dynamics is non-renormalizable: the Fibonacci map.

The dynamics of the real quadratic Fibonacci map, where the critical point returns closest to itself at the Fibonacci iterates, has been extensively studied (especially see [LM93]). Maps with Fibonacci type returns were first discovered in the cubic case by Branner and Hubbard [BH92] and have since been consistently explored because they are a fundamental combinatorial type of the class of non-renormalizable maps. The Fibonacci map was used by Lyubich and Milnor in developing the *generalized renormalization* procedure which has proven very fruitful. The Fibonacci map was also highlighted in the work of Yoccoz as it was in some sense the worst case in the proof of local connectivity of non-renormalizable Julia sets with recurrent critical point [Hub93], [Mil92].

The local connectedness proof of Yoccoz involves producing a sequence of partitions of the Julia set, now called Yoccoz puzzle pieces. These Yoccoz puzzle pieces are then shown to exhibit the *divergence property* and in particular nest down to the critical point, proving local connectivity there. Yoccoz then transfers this divergence property to the parapuzzle pieces around the parameter point to demonstrate

that the Mandelbrot set is locally connected at this parameter value. Lyubich further explores the Yoccoz puzzle pieces of Fibonacci maps and demonstrates that the *principal nest* of Yoccoz puzzle pieces has rescaled asymptotic geometry equal to the filled-in Julia set of $z \mapsto z^2 - 1$ and that the moduli of successive annuli grow at a linear rate [Lyu93b].

We prove that the same geometric and rescaling results hold for the principal nest of parapuzzle pieces for the Fibonacci parameter point in the Mandelbrot set. Let the notation $mod(A, B)$ (where $B \subset A$) indicate the modulus of the annulus $A \setminus B$. (See Appendix for the definition of the modulus.)

Theorem A: (Parapuzzle scaling and geometry)
The principal nest of Yoccoz parapuzzle pieces, P^n, for the Fibonacci point c_{fib} has the following properties.
1. They scale down to the point c_{fib} in the following asymptotic manner:

$$\lim_{n \to \infty} mod(P^{n-1}, P^n) \; / \; n = \frac{2}{3} \ln 2.$$

2. The rescaled P^n and the boundary of the rescaled P^n have asymptotic geometry equal to the filled-in Julia set of $z \mapsto z^2 - 1$ and its boundary, respectively.   By definition, the sets P^n, suitably rescaled,

have asymptotic geometry equal to a set K if there are complex affine transformations A_n so that the images $A_n(P^n)$ converge to K in the Hausdorff metric.

Remark. Concerning part 1 of Theorem A, we point out that in the paper [TV90], Tangerman and Veerman showed that in the case of circle mappings with a non-flat singularity, the parameter scaling and dynamical scaling agree for a large class of systems. They have real methods comparing the dynamical derivatives and parameter derivatives along the critical value orbit. Here, we use a complex technique for the unimodal scaling case since a direct derivative comparison appears to have extra difficulties. This is due to the changes in orientation, i.e., the folding which occurs for such maps, complicating the parameter derivative calculations.

Figures 1 and 2 illustrate item 2 of the theorem. The reader is also encouraged to compare Theorem A with Theorem 2.1 of Lyubich on page 10.

When dilating by the scaling factors given by the Fibonacci renormalization procedure, the computer pictures around the Fibonacci parameter also exhibit a hairy self-similarity. (Compare Figure 1 with Figure 7 on page 19.) Using the main construction of the proof of Theorem A, we demonstrate this hairiness. The appropriate scaling maps are denoted by R_n, and the Mandelbrot set by **M**.

Theorem B: (Hairiness for the Fibonacci parameter)
Given any disc $D(z, \epsilon)$ with center point z and radius $\epsilon > 0$, in the complex plane, there exists an N such that for all $n > N$ we have that

$$D(z, \epsilon) \cap R_n(\mathbf{M}) \neq \emptyset.$$

The text is organized as follows. In Section 1, we review some basic material of quadratic dynamics and the role of equipotentials and external rays. In Section 2, we review the generalized renormalization
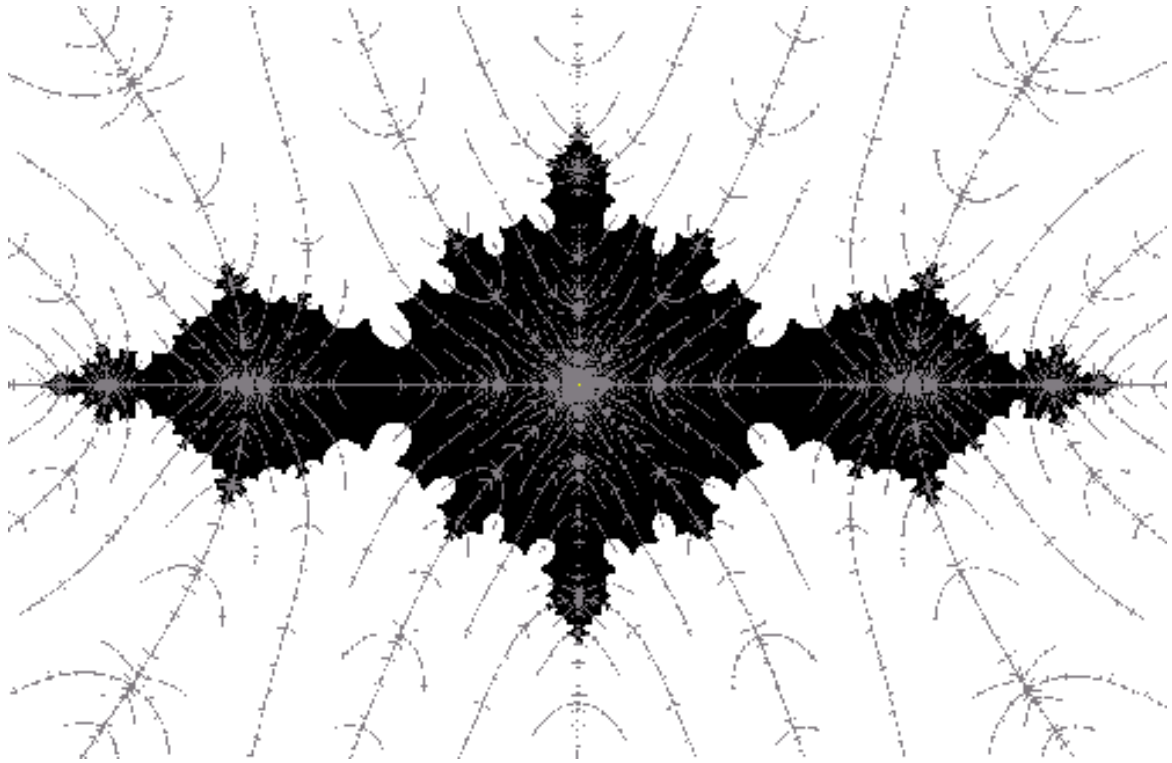
Figure 1: P^7 for the Fibonacci point, the seventh level parapuzzle piece with a part of the Mandelbrot set.

procedure, where we define the principle nest in the dynamical plane as well as in the parameter plane. In Section 3, we prove dynamical scaling and geometry results for the principal nest for parameter points which are Fibonacci renormalizable n-times. These results and proofs are analogous to those given by Lyubich ([Lyu93a], [Lyu93b]) for the Fibonacci point. In Section 4, we construct a map of parameter space which allows us to compare it to the dynamical space and prove Theorem A, part 2. In Section 5, we complete the proof of Theorem A. Finally, in Section 6 we prove Theorem B.

1   Introductory Material

We outline some of the basics of complex dynamics of quadratic maps from the Riemann sphere to itself so that we may build the puzzle and parapuzzle pieces. We will consider the normalized form, $f_c(z) = z^2 + c$ with parameter value $c \in \mathbb{C}$. The *basin of attraction* for infinity, $A(\infty)$, are all the points z which converge to infinity under iteration. The dynamics near infinity and the corresponding
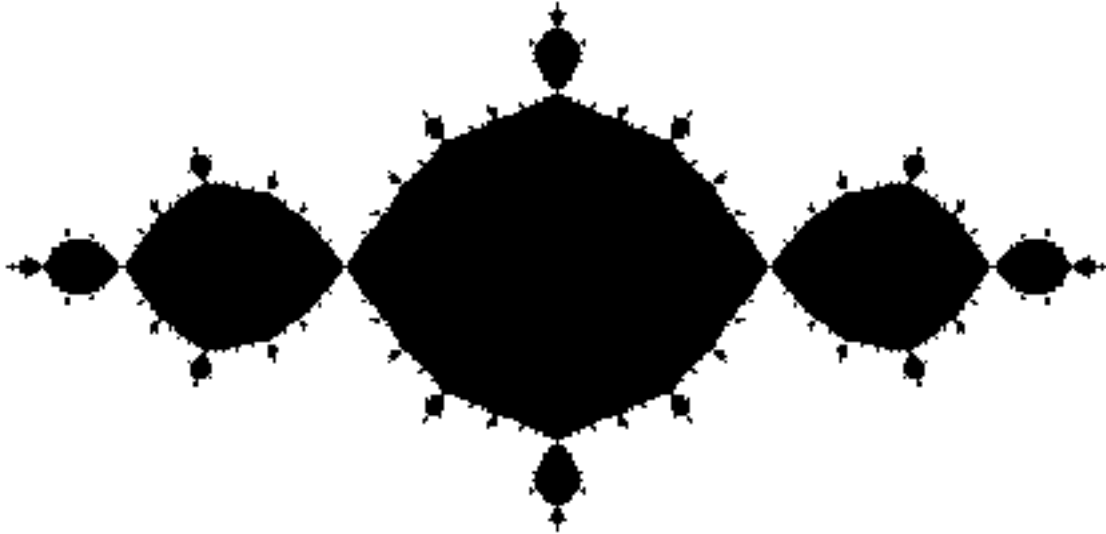
Figure 2: The filled-in Julia set of $z \mapsto z^2 - 1$.

basin of attraction has been understood since Böttcher (see [Mil90]). Notationally we have that $\mathbb{D}_r$ is the disc centered at 0 with radius r.

Theorem 1.1 *The map $f_c : A(\infty) \to A(\infty)$ is complex conjugate to the map $w \mapsto w^2$ near infinity. There exists a unique complex map Φ_c defined on $\widehat{\mathbb{C}} \setminus \bar{\mathbb{D}}_{r(c)}$, where $r(c)$ represents the smallest radius with the property that*

$$f_c \circ \Phi_c(w) = \Phi_c(w^2),$$

and normalized so that $\Phi_c(w) \sim w$ as $|w| \to \infty$.

By Brolin [Bro65] the conjugacy map Φ_c satisfies

$$\lim_{n \to \infty} \log^+(|f_c^n(z)|/2^n) = \log|\Phi_c^{-1}(z)|. \tag{1}$$

In fact, the left hand side of equation (1) is defined for all $z \in A(\infty)$ and is the Green's function for the Julia set.

   Equipotential curves are images of the circles with radii $r > r(c)$, centered at 0 in $\widehat{\mathbb{C}} \setminus \bar{\mathbb{D}}_r$ under the map Φ_c. Actually, the moment that the above conjugacy breaks down is at the critical point 0 if it is in $A(\infty)$. In this case, if we try to extend the above conjugacy we see that the image of the circle with radius $r(c)$ passing through the critical point is no longer a disc but a "figure eight". Despite the conjugacy difficulty, we may define equipotential curves passing through any point in $A(\infty)$ to be the level set from Brolin's formula. *External rays* are images of half open line segments emanating radially from $\mathbb{D}_{r(c)}$, i.e., $\Phi_c(re^{i\theta})$ with $r > r(c)$ and θ constant. In fact, these are the gradient lines

from Brolin's formula. So again, we may extend these rays uniquely up to the boundary of $A(\infty)$ or up to where the ray meets the critical point or some preimage, i.e., the "root" of a figure eight.

An external ray is referred to by its angle; for example the $\frac{1}{3}$-ray is the image of the ray with $\theta = \frac{1}{3}$. A central question to ask is whether a ray extends continuously to the boundary of $A(\infty)$. The following guarantees that some points (and their preimages) in the Julia set are such landing points.

Theorem 1.2 (Douady and Yoccoz, see [Mil90]) *Suppose z is a point in the Julia set which is periodic or preperiodic and the periodic multiplier is a root of unity or has modulus greater than 1, then it is the landing point of some finite collection of rays.*

One of the main objects of study in quadratic dynamics is the set of all parameters c such that the conjugacy Φ_c is defined for the whole immediate basin of infinity.

Definition. The *Mandelbrot set* **M** consists of all values c whose corresponding Julia set is connected.

The combinatorics of the Mandelbrot set have been extensively studied. In [DH85], Douady and Hubbard present many important results, some of which follow below.

Theorem 1.3 (Douady and Hubbard, [DH85])
1. The Mandelbrot set is connected.
2. The unique Riemann map $\Phi_M : \widehat{\mathbb{C}} \setminus \bar{\mathbb{D}} \to \widehat{\mathbb{C}} \setminus M$, with $\Phi_M(z) \sim z$ as $|z| \to \infty$, satisfies the following relation with the Böttcher map:

$$\Phi_M^{-1}(c) = \Phi_c^{-1}(c).$$

With the Riemann map Φ_M, we can define equipotential curves and external rays in the parameter plane analogous to the dynamical case above. From the second result of Theorem 1.3, it can be seen that the external rays and equipotentials passing through c (the critical value) in the dynamical space are combinatorially the same external rays and equipotentials passing through c in the parameter space. Since the Yoccoz puzzle pieces have boundary which include rays that land, it is essential for the construction of the parapuzzle pieces that these same external rays land in parameter space. Before stating such a theorem, we recall some types of parameter points. *Misiurewicz points* are those parameter values c such that the critical point of f_c is pre-periodic. A *parabolic point* is a parameter point in which the map f_c has a periodic point with multiplier some root of unity. For these points, their corresponding external rays land.

Theorem 1.4 (Douady and Hubbard, [DH85]) *If c is a Misiurewicz point then it is the landing point of some finite collection of external rays $R_M(\theta_i)$, where the θ_i represent the angle of the ray. In the dynamical plane, external rays of the same angle, $R_{f_c}(\theta_i)$, land at c (the critical value of f_c).*

Theorem 1.5 (Douady and Hubbard, [DH85]) *If c is a parabolic point then it is the landing point of two external rays (except for $c = \frac{1}{4}$ which has one landing ray). In the dynamical plane for this c, these external rays land at the root point of the Fatou component containing the critical value.*

Using rays and equipotentials in dynamical space, Yoccoz developed a kind of Markov partition, now called Yoccoz puzzle pieces, for non-renormalizable (or at most finitely renormalizable) Julia sets with recurrent critical point and no neutral cycles [Hub93]. Combining Theorems 1.3 and 1.4, Yoccoz constructed the same (combinatorially) parapuzzle pieces for the parameter points of the non-renormalizable maps.

For our purposes we will now focus on the maps exhibiting initial behavior similar to the dynamics of the Fibonacci map. The Fibonacci parameter value lies in what is called the $\frac{1}{2}$-wake. The $\frac{1}{2}$-wake is the connected set of all parameter values with boundary consisting of the $\frac{1}{3}$- and $\frac{2}{3}$-rays (which meet at a common parabolic point) and does not contain the main cardioid. Dynamically, all such parameter points have a fixed point which is a landing point for the same angle rays, $\frac{1}{3}$ and $\frac{2}{3}$. In fact, for all parameter points in the $\frac{1}{2}$-wake, the two fixed points are stable; we may follow them holomorphically in the parameter c. We are now in a good position to review generalized renormalization in the $\frac{1}{2}$-wake. We point out that this procedure, developed in [Lyu93a], is not restricted to the $\frac{1}{2}$-wake and the construction given below is readily generalized from the following description.

2 A Review of Puzzles and Parapuzzles

Initial Yoccoz Puzzle Pieces

We now review the Yoccoz puzzle piece construction essentially without proofs. (See [Hub93] or [Lyu93a] for more details.) For each parameter in the $\frac{1}{2}$-wake, we begin with the two fixed points commonly called the α and β fixed points. The β fixed point is the landing point of the $0 - ray$ (the only ray which maps to itself under one iterate). The α point is the landing point of the $\frac{1}{3}$- and $\frac{2}{3}$-rays for all parameters in the $\frac{1}{2}$-wake. By the Böttcher map, it is easy to see that the $\frac{1}{3}$- and $\frac{2}{3}$-rays are permuted by iterates of f_c. The initial Yoccoz puzzle pieces are constructed as follows. Fix an equipotential E. The top level Yoccoz puzzle pieces are the bounded connected sets in the plane with boundaries made up of parts of the equipotential E and external rays. (See Figure 3.) For the generalized renormalization procedure described below, the top level Yoccoz puzzle piece containing the critical point is labeled V_0^0.

The Principal Nest

The generalized renormalization procedure for quadratic maps with recurrent critical point proceeds as follows. For each parameter value c, iterate the critical point 0 by the map f_c until it first returns back to the set V_0^0. In fact, this will be two iterates. Take the largest connected set around 0, denoted V_0^1, such that $f^2(V_0^1) = V_0^0$. Note that we suppress the parameter c in this discussion, $V_0^n = V_0^n(c)$. This is the level 1 central puzzle piece and we label the return map f_c^2 restricted to the domain V_0^1 by g_1 $(= g_{1,c})$. It is easy to see that $V_0^1 \subset V_0^0$ and that g_1 is a two-to-one branched cover. The boundary of V_0^1 is made up of pieces of rays landing at points which are preimages of α, as well as pieces of some fixed equipotential. Now we proceed by induction. Iterate the critical point until it first returns to V_0^n, say in m iterates, and then take the largest connected set around 0, denoted V_0^{n+1}. This gives $f_c^m(V_0^{n+1}) = V_0^n$. Inductively we get a collection of nested connected sets $V_0^0 \supset V_0^1 \supset V_0^2 \supset V_0^3...$, and return maps $g_n(V_0^n) = V_0^{n-1}$. Each of the V_0^i has boundary equal to some collection of pieces of rays landing at preimages of α and pieces of some equipotential. Each g_i is a two-to-one branched cover. The collection of V_0^i is called the *principal nest* of Yoccoz puzzle pieces
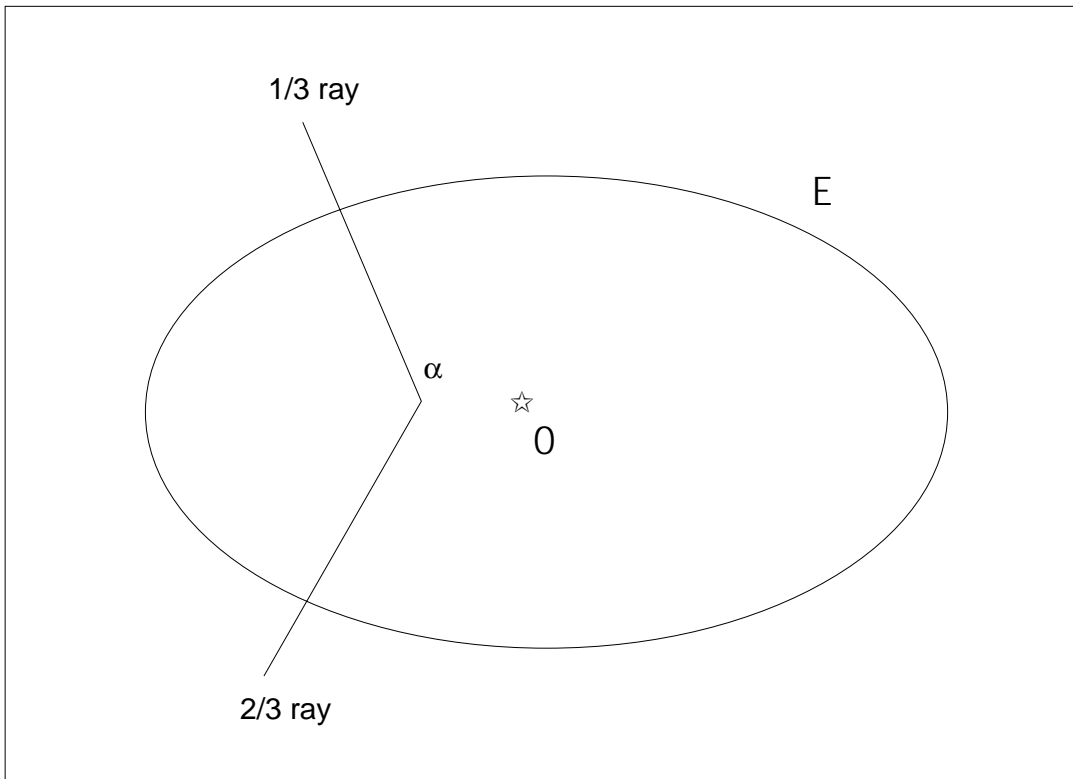
Figure 3: Beginning generalized renormalization.

around the critical point.

To define the principal nest of Yoccoz parapuzzle pieces in the parameter space it is easiest to view the above procedure around the critical value. In this case, the principal nest is just the image of the principal nest for the critical point, namely $f_c(V_0^0) \supset f_c(V_0^1) \supset f_c(V_0^2) \supset f_c(V_0^3)$.... Notice that again the puzzle pieces are connected and we have that the boundary of each puzzle piece to be some parts of a fixed equipotential and parts of some external rays landing at preimages of α. If we consider these same combinatorially equipotentials and external rays in the parameter space we get a nested collection of Yoccoz parapuzzle pieces. By combinatorially the same we mean external rays with the same angle and equipotentials with the same values.

Definition. Given a parameter point c, the *parapuzzle piece of level n*, denoted by $P^n(c)$, is the set in parameter space whose boundary consists of the same (combinatorially) equipotentials and external rays as that of $f_c(V_0^n)$.

We mention the essential properties about the sets P^n used by Yoccoz. (The reader may wish to consult [Hub93] or [GM93].) The sets P^n are topological discs. For all points c in P^n, the Yoccoz puzzle pieces of the principal nest (up to level n) are combinatorially the same. This structural stability also applies to the off-critical pieces (up to level n) which are defined below. Hence, all parameter points in P^n may be renormalized in the same manner combinatorially up to level n. We also point out that the set P^n ($n > 0$) intersects the Mandelbrot set only at Misiurewicz points.

Off-critical Puzzle Pieces

If a quadratic map is non-renormalizable, then at some level the principal nest is non-degenerate. In other words, there is some N such that for all $n \geq N$, $\mathrm{mod}(V_0^n, V_0^{n+1})$ is non-zero. For these same $n \geq N$, we may iterate the critical point by the map g_n some finite number of times until landing in $V_0^{n-1} \setminus V_0^n$ (otherwise the map would be renormalizable). Hence, to keep track of the critical orbit the generalized renormalization incorporates the following procedure. Let us fix a level n. For any point x in the closure of the critical orbit contained in $V_0^{n-1} \setminus V_0^n$, we iterate by f_c until it first returns back to the V_0^{n-1} puzzle piece. Denoting the number of iterates by l, we then take the largest connected neighborhood of x, say X, such that $f^l(X) = V_0^{n-1}$. We only save those sets X, denoted V_i^n $(i > 0)$, which intersect some point of the critical orbit. We point out that the collection of V_i^n are pairwise disjoint for $n > 1$. The return map $f^l(V_i^n)$ restricted to the set V_i^n will still be denoted by g_n. The boundary of each V_i^n must be a union of external rays landing at points which are some preimage of α and pieces of some equipotential. Also, the return maps g_n restricted to V_i^n $(i \neq 0)$ are univalent. To review, for each level n we have a collection of disjoint puzzle pieces V_i^n and return maps,

$$\bigcup_i V_i^n \subset V_0^n,$$
$$g_n(V_i^n) = V_0^n.$$

The Fibonacci Combinatorics

Let us denote the Fibonacci sequence by $u(n)$, where $u(n)$ represents the n-th Fibonacci number. The Fibonacci numbers are defined inductively: $u(0) = 1, u(1) = 1$ and $u(n) = u(n-1) + u(n-2)$. The dynamical condition for $f_{c_{fib}}$ (recall c_{fib} is real) is that for all Fibonacci numbers $u(n)$, we have $|f^{u(n)}(0)| < |f^{u(n-1)}(0)| < |f^i(0)|$, $u(n-1) < i < u(n)$. So the Fibonacci combinatorics require that the critical point return closest to itself at the Fibonacci iterates.

The generalized renormalization for the Fibonacci case is as follows. (See [LM93] and [Lyu93b] for a more detailed account. There is only one off-critical piece at every level, V_1^n. The return map of V_1^n to V_0^{n-1} is actually just the restriction of the map $g_{n-1} : V_0^{n-1} \to V_0^{n-2}$. We point out that the map g_{n-1} is the iterate $f^{u(n)}$ with restricted domain. In short we have

$$g_n \, (\simeq g_{n-2} \circ g_{n-1}) \quad : \quad V_0^n \to V_0^{n-1} \quad (analytic\ double\ cover),$$
$$g_{n-1} \quad : \quad V_1^n \to V_0^{n-1} \quad (univalent).$$

Finally, we define the puzzle piece $\widetilde{V}_1^{n+1}$ to be the set V_1^{n+1} which map to the central puzzle piece of the next level down under g_n. Namely, $\widetilde{V}_1^{n+1}$ is the set such that

$$\widetilde{V}_1^{n+1} \subset V_1^{n+1},$$
$$g_n(\widetilde{V}_1^{n+1}) = V_0^{n+1}.$$
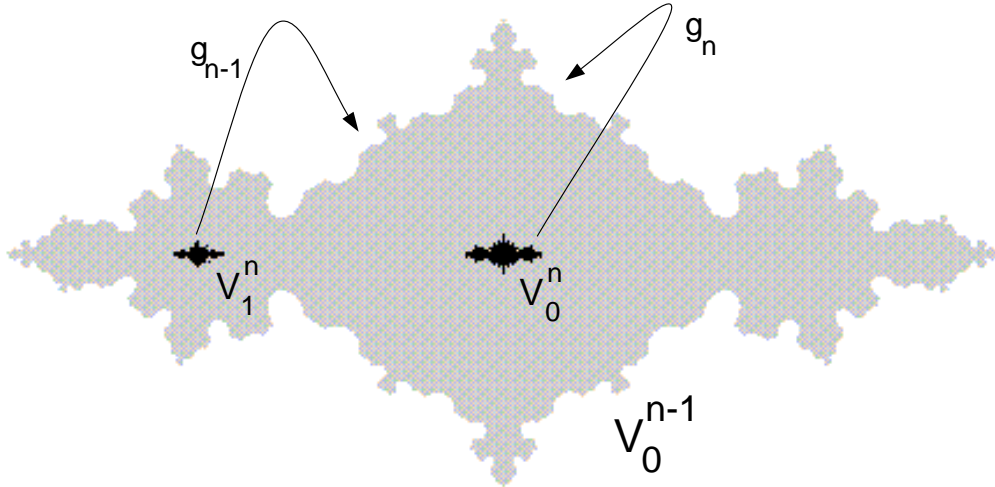
Fibonacci Parapuzzle Pieces

Figure 4: Generalized renormalization: Fibonacci type return with $n = 7$.

A Fibonacci parapuzzle piece, P^n, is defined as the set with the same combinatorial boundary as that of $f(V_0^n)$. We also define an extra puzzle piece, Q^n. In particular, Q^n is a subset of P^{n-1} and hence may be renormalized in the Fibonacci way $n-1$ times. The boundary of the set Q^n is combinatorially the same as $f(V_1^{n-1})$. Finally observe that $P^n \subset Q^n \subset P^{n-1}$. Properties for P^n and Q^n are given below.

$$c \in P^n \implies g_n(0) \in V_0^{n-1}$$
$$c \in Q^{n+1} \implies g_n(0) \in V_1^n$$
$$c \in P^{n+1} \implies g_n(0) \in \widetilde{V}_1^n$$

We warn the reader that the parameter value c has been suppressed as an index for the maps g and puzzle pieces V. Also, it is useful to use Figure 4 when tracing through the above properties of Q^n, P^n, and P^{n+1}, keeping in mind that $\widetilde{V}_1^n$, although too small for this picture, is contained in V_1^n (see Figure 5).

Lyubich's Motivating Result

The main motivating result of Lyubich is stated below. We will give a brief review of the proofs and also point out that the proof of part 2 of the theorem may be found in Lemma 4 of [Lyu93b], while the proof of part 1 is a direct consequence of part 2 and the scaling results of [Lyu93a] (see pages
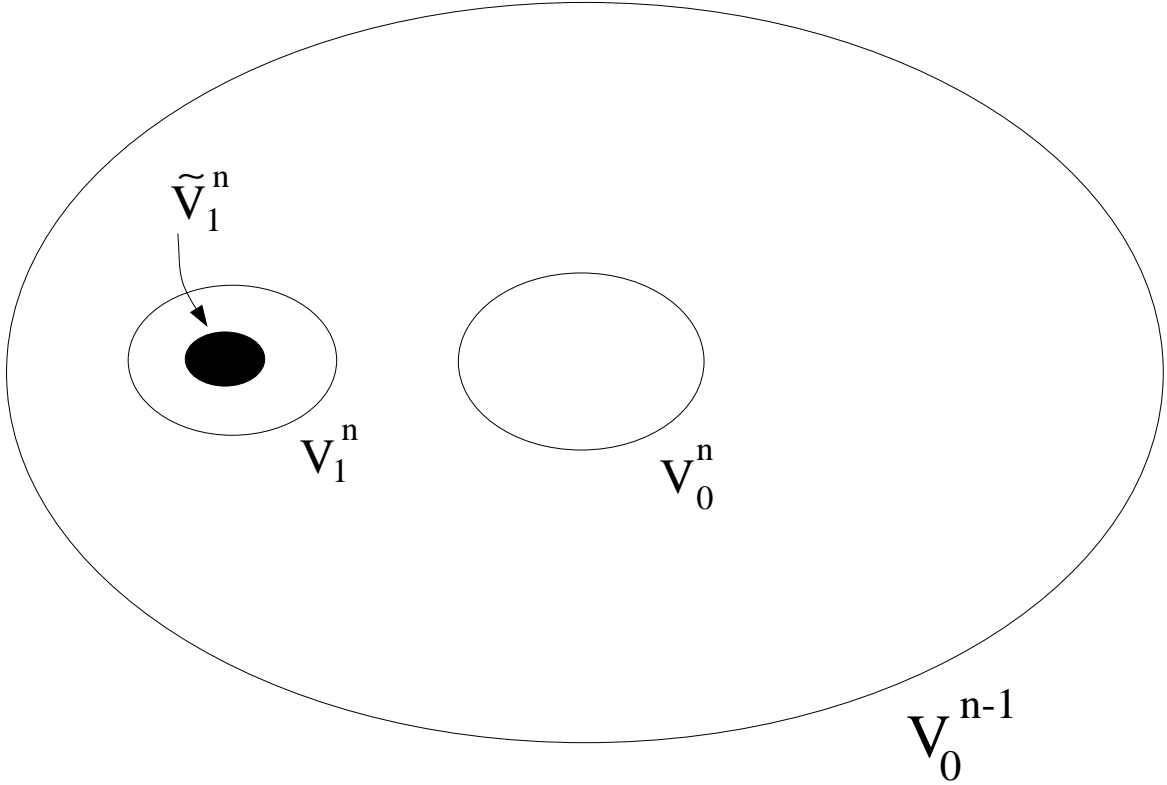
9

Figure 5: Fibonacci puzzle piece nesting.

11-12 of this paper). Finally, we point out that similar scaling results were obtained on the real line in Lemma 5.4 of [LM93].

Theorem 2.1 (Lyubich) *The principal nest of central Yoccoz puzzle pieces for the Fibonacci map has the following properties.*
1. The puzzle pieces scale down to the critical point in the following asymptotic manner:

$$\lim_{n \to \infty} \mathrm{mod}(V_0^{n-1}, V_0^n) \, / \, n = \frac{1}{3} \ln 2.$$

2. The rescaled puzzle pieces V_0^n have asymptotic geometry equal to the filled-in Julia set of $z \mapsto z^2 - 1$.

The scaling factor in the theorem is exactly half that for the parameter scaling. This is because here the scaling is done around the critical point as opposed to the critical value.

3   Beginning Geometry and Scaling

In studying the parameter space of complex dynamics, one first needs a strong command of the dynamics for all the parameter points involved. Hence, before proceeding in the parameter space we shall first study the geometry of the central puzzle pieces, $V_0^n(c)$, for all $c \in Q^n$.

10

Before stating a result similar to Theorem 2.1 for $c \in Q^n$, we indicate precisely how the rescaling of $V_0^n(c)$ is to be done. For the parameter point c_{fib}, we dilate (about the critical point) the set $V_0^n(c_{fib})$ by a positive real constant so that the boundary of the rescaled $V_0^n(c_{fib})$ intersects the point $(1 + \sqrt{5})/2$, the non-dividing fixed point for the map $z^2 - 1$. If we dilate all central puzzle pieces $V_0^n(c_{fib})$ this way, we can then consider the rescaled return maps of g_n, denoted G_n, which map the dilated $V_0^n(c_{fib})$ to the dilated $V_0^{n-1}(c_{fib})$ as a two-to-one branched cover. The map G_n restricted to the real line either has a minimum or maximum at the critical point. To eliminate this orientation confusion, let us always rescale (so now possibly by a negative number) $V_0^n(c_{fib})$ so that the map G_n always has a local minimum at the critical point.

The point which maps to $(1 + \sqrt{5})/2$ for $V_0^n(c_{fib})$ under this dilation we label β_n. Note that it must be some preimage of our original fixed point α and hence a landing point of one of the boundary rays. (Puzzle pieces may only intersect a Julia set at preimages of α.) This point β_n is parameter stable in that it may be continuously (actually holomorphically) followed for all $c \in Q^{n+1}$. Hence we may write $\beta_n(c)$. So for $c \in Q^{n+1}$, the rescaling procedure for $V_0^n(c)$ is to linearly scale (now possibly by a complex number) by taking $\beta_n(c)$ to $(1 + \sqrt{5})/2$.

The geometric lemma below gives asymptotic structure results for the central puzzle pieces $V_0^n(c)$ for all $c \in Q^n$. In particular, the lemma indicates that as long as we can renormalize, the rescaled central puzzle pieces converge to the Julia set of $z^2 - 1$. The notation $J\{z^2 - 1\}$ is used to indicate the Julia set for the map $z \mapsto z^2 - 1$.

Before proceeding we give a brief review of the Thurston Transformation (see [DH93]) needed in the next lemma. Consider the Riemann sphere punctured at $\infty, -1, 0$, and $\frac{1+\sqrt{5}}{2}$. The map $\theta : z \mapsto z^2 - 1$ fixes ∞ and $\frac{1+\sqrt{5}}{2}$ while -1 and 0 form a two cycle. Consider any conformal structure ν on the Riemann sphere punctured at these points. We can pull this conformal structure back by the map θ. This induces a map T on the Teichmüller space of the four punctured sphere. A main result of this transformation T is as follows.

Theorem 3.1 (Thurston) *Given any conformal structure ν we have that $T^n(\nu)$ converges at exponential rate to the standard structure in the Teichmüller space.*

Lemma 3.2 (Geometry of central puzzle pieces) *Given $\epsilon > 0$, there exists an $N > 0$ such that for all $c \in Q^i$ where $i \geq N$ we have that the rescaled $\partial V_0^j(c)$ is ϵ-close in the Hausdorff metric around $J\{z^2 - 1\}$, where $i \geq j + 1 \geq N$.*

Proof: First observe that the Julia set for $\Theta : z \mapsto z^2 - 1$ is hyperbolic. This means that given a small δ-neighborhood of the Julia set there is some uniform contraction under preimages. More precisely, there exists an integer m and value $K > 1$ such that for any point in the δ-neighborhood of $J\{z^2 - 1\}$ we have

$$\max_{y \in \Theta^{-m}(x)} \text{dist}(y, J\{z^2 - 1\}) < \frac{1}{K} \text{dist}(x, J\{z^2 - 1\}). \qquad (2)$$

Returning to our Fibonacci renormalization, it is a consequence of the main theorem of Lyubich's paper [Lyu93a] that the moduli of the nested central puzzle pieces, i.e., $\text{mod}(V_0^n, V_0^{n-1})$, grow at least at a linear rate independent of c. Hence, independent of our parameters c (although we must be able

to renormalize in the Fibonacci sense), we have a definite growth in Koebe space for the map g_n. (This is somewhat misleading as the map g_n is really a quadratic map composed with some univalent map. Thus, when we say the map g_n has a large Koebe space, we really mean that the univalent return map has a large Koebe space.) The growing Koebe space implies that the rescaled maps $G_{n,c}$ have the following asymptotic behavior:

$$G_{n,c}(z) = (z^2 + k(n,c))(1 + O(p^n)). \tag{3}$$

The bounded error term $O(p^n)$ comes from the Koebe space and hence, by the above discussion, is independent of c.

We claim that $k(n,c) \to -1$ at an exponential rate in n, i.e., $|k(n,c) + 1|$ exponentially decays. This result was shown to be true for $k(n, c_{fib})$ in Lemma 3 of [Lyu93b]. We use this result as well as its method of proof to show our claim. First, we review the method of proof used by Lyubich in the Fibonacci case. This was to apply Thurston's transformation on the tuple ∞, $G_n(0)$, 0, and $\frac{1+\sqrt{5}}{2}$. Pulling back this tuple by G_n results in a new tuple: ∞, the negative preimage of $G_n^{-1}(0)$, 0, and $\frac{1+\sqrt{5}}{2}$. Next, two facts are used concerning the negative preimage of $G_n^{-1}(0)$. The first is that it is bounded between 0 and $-\frac{1+\sqrt{5}}{2}$. (This is shown in [LM93].) The second is that the puzzle piece V_1^{n+1} is exponentially small compared to V_0^n (a consequence of the main result of [Lyu93a]); therefore, after rescaling, the points $G_n^{-1}(0)$ and $G_{n+1}(0)$ are exponentially close. Hence, the tuple map

$$\left(\infty, G_n(0), 0, \frac{1+\sqrt{5}}{2}\right) \mapsto \left(\infty, G_{n+1}(0), 0, \frac{1+\sqrt{5}}{2}\right) \tag{4}$$

is exponentially close to the Thurston transformation since the pull-back by G_n is exponentially close to a quadratic pull-back map (in the C^1 topology). The Thurston transformation is strictly contracting; hence, the tuple must converge to its fixed point $(\infty, -1, 0, \frac{1+\sqrt{5}}{2})$. Hence, we get $k(n, c_{fib}) \to -1$ at a uniformly exponential rate. This concludes the summation of the Fibonacci case.

To prove a similar result for our parameter values c, let us choose some large level n for which the c_{fib} tuple is close to its fixed point tuple and such that the Koebe space for g_n is large, i.e., $G_{n,c}$ is very close to a quadratic map. Then we can find a small neighborhood around c_{fib} in parameter space for which we still have a large Koebe space for g_n (notationally g_n is now c dependent) and its respective tuple is also close to the fixed point tuple. Then as long as the values c in this neighborhood are Fibonacci renormalizable, we claim the $|k(n,c) + 1|$ exponentially decays. We know that the Koebe space growth is at least linear and independent of the value c; hence by the strict contraction of the Thurston transformation we get our claim of convergence for $k(n,c)$. Thus we may replace Equation (3) with

$$G_{n,c}(z) = (z^2 - 1)(1 + O(p^n)). \tag{5}$$

Returning to Equation (2), we can state a similar contraction for the maps $G_{n,c}$. In particular, in some small δ-neighborhood of $J\{z^2 - 1\}$, we can find a value k ($K > k > 1$) and large positive integer N_1 so that for the same value m as in Equation (2) and for all $n > N_1$, we have

$$\max_{y \in G_{n+m-1,c}^{-1} \circ G_{n+m-2,c}^{-1} \circ \ldots \circ G_{n,c}^{-1}(x)} \mathrm{dist}(y, J\{z^2 - 1\}) < \frac{1}{k}\mathrm{dist}(x, J\{z^2 - 1\}), \tag{6}$$

as long as c is renormalizable in the Fibonacci sense, i.e., $n + m$ times.

From Equation (6), we conclude the lemma. We take the rescaled V_0^n and note that it contains the critical point and critical value. Hence we see that the topological annulus with boundaries $\partial \mathbb{D}_r$, r large, and ∂V_0^n under pull backs of $G_{n,c}$ must converge to the required set. This concludes the lemma. $\odot$

The geometry of the puzzle pieces provides us with sufficient dynamical scaling results for the central puzzle pieces as well as for the off-critical puzzle pieces for $c \in Q^n$.

Lemma 3.3 *Given $\epsilon > 0$ there exists an N so that for all $c \in Q^n$, $n > N$, we have the following asymptotics for the moduli growth of the principal nest*

$$\left| \frac{\mod(V_0^n(c), V_0^{n+1}(c))}{n} - \frac{1}{3} \ln 2 \right| < \epsilon. \tag{7}$$

Proof: Notationally we will suppress the dependence of the parameter c. By Lyubich ([Lyu93a], page 12), the moduli growth from $\mod(V_0^{n-1}, V_0^n)$ to $\mod(V_0^n, V_0^{n+1})$ approaches $\frac{1}{2}(-\text{cap}_\infty(J\{z^2 - 1\}) - \text{cap}_0(J\{z^2 - 1\}))$. (See Appendix for the definition of capacity.) The proof of the growth relies only on the geometry of the puzzle pieces. The map g_n takes the annulus $V_0^n \setminus V_0^{n+1}$ as a two-to-one cover onto the annulus $V_0^{n-1} \setminus \widetilde{V}_1^n$. Hence we have the equality

$$\mod(V_0^n, V_0^{n+1}) = \frac{1}{2}\mod(V_0^{n-1}, \widetilde{V}_1^n). \tag{8}$$

Using the Grötzsch inequality on the right hand modulus term, we have

$$\mod(V_0^{n-1}, \widetilde{V}_1^n) = \mod(V_0^{n-1}, V_1^n) + \mod(V_1^n, \widetilde{V}_1^n) + a(V_0^{n-1}, \widetilde{V}_1^n), \tag{9}$$

where the function $a(V_0^{n-1}, \widetilde{V}_1^n)$ represents the Grötzsch error. By applying the map g_{n-1} to V_1^n we see that $\mod(V_1^n, \widetilde{V}_1^n)$ is equal to $\mod(V_0^{n-1}, V_0^n)$. The term $\mod(V_0^{n-1}, V_1^n)$ converges to $\mod(V_0^{n-2}, V_0^{n-1})$. This is easily seen by applying the map g_{n-1} which is a two-to-one branched cover with the critical point image being pinched away from V_0^{n-1} as $n \to \infty$. Finally, the Grötzsch error a depends only on the geometry of V_0^n because of the linear increase in modulus between both V_0^{n-1} and V_0^{n+1} and hence is approaching $-\text{cap}_\infty(V_0^n) - \text{cap}_0(V_0^n)$ (see Lemma A.2 in the Appendix). But this is approaching $-\text{cap}_\infty(J\{z^2 - 1\}) - \text{cap}_0(J\{z^2 - 1\})$ by Lemma 3.2 and the fact that the capacity function preserves convergence in the Hausdorff metric (see Lemma A.1). Finally, $-\text{cap}_\infty(J\{z^2 - 1\}) - \text{cap}_0(J\{z^2 - 1\})$ is shown to be equal to $\ln 2$ in the Appendix. Using the notation $m_n = \mod(V_0^{n-1}(c), V_0^n(c))$, we may rewrite Equation (9) as

$$m_{n+1} = \frac{1}{2}m_n + \frac{1}{2}m_{n-1} + \frac{1}{2}a + o(1),$$

where $a = \ln 2$. The asymptotics of this equation give the desired result. $\odot$

4   The Parameter Map

Dynamical puzzle piece rescaling

Now that we have a handle on the geometry of the central puzzle pieces for values c in our parapuzzle, let us consider rescaling the V_0^n in a slightly different manner. For each $c \in Q^n$ dilate V_0^n so that the point $g_n^{-1}(0)$ maps to -1. Notice this is just an exponentially small perturbation of our previous rescaling since there we had $G_n^{-1}(0)$ approaching -1 uniformly in n for all $c \in Q^n$. Hence Lemmas 3.2 and 3.3 still hold for this new rescaling. Let us denote this new rescaling map by $r_{n,c}$. Therefore, fixing $c \in Q^n$, the map $r_{n,c}$ is the complex linear map $x \mapsto (1/g_n^{-1}(0)) \cdot x$.

Lemma 4.1 *The rescaling map $r_{n,c}$ is analytic in c. In other words, $g_n^{-1}(0)$ is analytic in $c \in Q^n$.*

Proof: The roots of any polynomial vary analytically without branching provided no two collide. We claim the root in question does not collide with any other. But for all $c \in Q^n$ we have that the piece $V_1^{n+1}(c)$ can be followed univalently in c. Hence, we have our claim. $\odot$

We remind the reader that the map $g_{n,c}$ is just a polynomial in c. Let us define the analytic parameter map which allows us to compare the dynamical space and the parameter space.

The Parameter Map: The map $M_n(c)$ is defined as the map $c \mapsto r_{n,c} \cdot g_{n+1,c}(0)$ with domain $c \in Q^n$.

Since the map $r_{n,c}$ is just a dilation for fixed c, we see that if $M_n(c) = 0$ then this parameter value must be superstable. This superstable parameter value, denoted c_n, is the unique point which is Fibonacci renormalizable n times, and for the renormalized return map, the critical point returns precisely back to itself, i.e., $g_n(0) = 0$. Equivalently, this is the superstable parameter whose critical point has closest returns at the Fibonacci iterates until the $n + 1$ Fibonacci iterate when it returns to itself, $f_{c_n}^{u(n+1)}(0) = 0$.

Lemma 4.2 (Univalence of the parameter map.) *For sufficiently large n, there exists a topological disc S^n such that $P^n \subset S^n \subset Q^n$, the map $M_n(c)$ is univalent in S^n, and $\mathrm{mod}(S^n, P^n)$ grows linearly in n.*

The proof of Lemma 4.2 is technical so we give an outline for the reader's convenience. We first show that the winding number is exactly 1 around the image -1 for the domain P^n. This will be a consequence of analysis of a finite number of Misiurewicz points along the boundary of P^n. Using Lemma 3.2 we will locate the positions (up to some small error) these selected Misiurewicz points must map to under $M_n(c)$. Then we prove that the image of the segments in ∂P^n between these Misiurewicz points is small, where "between" is defined by the combinatorial order of their rays and equipotentials. Hence, the $c \in \partial P^n$ have to follow the combinatorial order of the points of $J\{z^2 - 1\}$ without much error. Since we wind around -1 only once when traveling around $J\{z^2 - 1\}$ the only way we could have more than one preimage of -1 for the map $M_n(c)$ would be for one of these segments of ∂P^n to stretch a "large" distance and go around the point -1 a second time. But this cannot happen if the segments follow the order of $J\{z^2 - 1\}$ without much error. Finally, we show that this degree one property extends to some increasingly large image around -1 in Lemma 4.3.

Proof: We will again use the map $\Theta(z) = z^2 - 1$. Let $b_0 = \frac{1+\sqrt{5}}{2}$ be the non-dividing fixed point for the Julia set of Θ. The landing ray for this point is the 0-ray. Taking a collection of pre-images of

b_0 under the map Θ we may order them by the angle of the ray that lands at each point. (Note that there is only one angle for each point.) The notation for this combinatorial order of preimages will be $b_0, ... b_i, b_{i+1}, ..., b_0$.

Since the point b_0 is in the Julia set of Θ, the set of all preimages of b_0 is dense in the Julia set. Given that this Julia set is locally connected we have the following density property of the preimages of b_0: given any $\epsilon > 0$, we can find an l so that the collection of preimages $\Theta^{-l}(b_0)$ is such that the Julia set between any two successive points (in combinatorial order) is compactly contained in an ϵ-ball. In other words, for this set $\Theta^{-l}(b_0)$, given any b_i and b_{i+1}, the combinatorial section of the Julia set of Θ between these two points is compactly contained in an ϵ-ball.

For each $c \in Q^n$ we define an analogous set of points $b_{i,n}(c)$ along the boundary of the rescaled puzzle pieces $V_0^n(c)$. First let us return to our old way of rescaling $V_0^n(c)$, taking the point $\beta_n(c)$ to $1 + \sqrt{5}/2$ (see page 11). For our value l above we take a set of points to be preimages of $(1 + \sqrt{5})/2$ under the map $G_{n-1} \circ ... \circ G_{n-l}$ for each c. These points are on the boundary of the rescaled $V_0^n(c)$ and in particular are endpoints of some of the landing rays which make up some of the boundary of the rescaled V_0^n. In particular, we may label and order this set of preimages $b_{i,n}(c)$ by the angles of their landing rays. Hence we may also refer to a piece of the rescaled boundary of $V_0^n(c)$ as a piece of the boundary that is combinatorially between two successive $b_{i,n}(c)$.

We claim that for n large enough we have that for all $c \in Q^n$ these combinatorial pieces of $r_{n,c}(V_0^n)$, say from $b_{i,n}$ to $b_{i+1,n}$, is in the exact same ϵ-ball as their b_i to b_{i+1} piece counterpart. For this claim we first want $b_{i,n}(c) \to b_i$ as $n \to \infty$. But this is true (for this rescaling) by the proof of Lemma 3.2 since the rescaled maps G_n converge to Θ exponentially.

Now that we have a nice control of where the Misiurewicz points of ∂P^n are landing, we focus on the boundary segments of P^n between them. Note that by Theorem 1.3 of Douady and Hubbard, we have a good combinatorial description of ∂P^n in terms of rays and equipotentials. Combinatorially the image of these boundary segments under the map M_n will be in the appropriate boundary segments of the dynamical puzzle pieces. Therefore, we focus on controlling the combinatorial segments between the $b_{i,n}$ along the central puzzle pieces in dynamical space. With precise information on where these combinatorial segments are in dynamical space we make conclusions on the image of ∂P^n.

Now we prove that the combinatorial piece between $b_{i,n}(c)$ and $b_{i+1,n}(c)$ converges to the combinatorial piece from b_i to b_{i+1} in the Hausdorff metric. Let us take a small neighborhood around c_{fib} such that the rescaled V_0^n are in some small neighborhood around $J\{z^2 - 1\}$. For all c in this neighborhood, take the combinatorial piece $b_{i,n}(c)$ to $b_{i+1,n}(c)$ such that the distance (in the Hausdorff metric) is greatest from b_i to b_{i+1}. Suppose this distance is δ, then after m preimages (the value m being the same as in Lemma 3.2, see Equations (2) and (6)), the distances between these preimages is less than δ/λ^m, where $\lambda > 1$ and is independent of the parameter. Finally, notice that for the b_i segments, any preimages of a combinatorial segment must be contained in another b_i segment (the Markov property). Hence, we actually get convergence at an exponential rate.

To review, the points $c \in \partial P^n$ under the map $M_n(c)$ must traverse around the point -1 with each appropriate Misiurewicz point landing very near b_i since for all c, $b_{i,n}(c) \to b_i$. But each combinatorial piece is also very near the combinatorial piece for the Julia set of Θ and the Julia set has winding number 1 around the point -1 which completes the winding number argument for this rescaling. Now if we rescale by $r_{n,c}$ instead of the old way (they are exponentially close) the same result holds. This completes the proof of the univalence of the map at least in some small image containing -1. The

lemma below will complete the proof of this lemma. $\odot$

Lemma 4.3 *For all sufficiently large n, there exists $R(n) \to \infty$ as $n \to \infty$ such that the map $c \mapsto M_n(c)$ is univalent onto the disc $D(-1, R(n))$.*

Proof: The image of any point $c \in \partial Q^n$ under the map $M_n(c)$ is contained in the set $r_{n,c}(V_0^{n-1}(c))$. But the boundary of $r_{n,c}(V_0^{n-1}(c))$ under the rescaling of $r_{n,c}$ is very far from $r_{n,c}(V_0^n(c))$ by the modulus growth proven in Lemma 3.3 (see Appendix, Proposition A.3 and reference). Let R equal the minimum distance from the image of ∂Q^n to the origin. Note that $Q^n \setminus P^n$ cannot contain the point -1 in its image under $M_n(c)$ since the closest these points can map to -1 is when they map into a small neighborhood of $J\{z^2 - 1\}$. Since we showed in the proof above that the winding number around -1 for $M_n(\partial P^n)$ is one, we must have the same result for $M_n(\partial Q^n)$ since -1 can have no new preimages in this domain $Q^n \setminus P^n$. Hence, the winding number is one for all points in the disc of radius R. Thus, the map M_n must be univalent in some domain with image (at least) the disc centered at 0 and radius R. Taking the preimage of this disc will define the desired set in parameter space, S^n. The result follows and hence does Lemma 4.2. $\odot$

Lemma 4.2 also allows us to give the geometric result of Theorem A. As n increases we have an increasingly large Koebe space around the image of ∂P^n. Since the image of ∂P^n under the map $M_n(c)$ must asymptotically approach that of $J\{z^2 - 1\}$, the parapuzzle pieces must also asymptotically approach this same geometry by application of the Koebe Theorem. Hence, by Lemma 4.2, we get part 2 of Theorem A.

5 Parapuzzle Scaling Bounds

To understand the scaling in parameter space, we focus on the image of the parapuzzle pieces P^n and P^{n+1} under the parameter map M_n. Since M_n is nearly a linear map for the domain P^n, we are in a good position to prove the scaling results of the Main Theorem A.

Theorem 5.1 (Theorem A, part 1.) *The principal nest of Yoccoz parapuzzle pieces P^n for the Fibonacci point c_{fib} scale down in the following asymptotic manner:*

$$\lim_{n \to \infty} \text{mod}(P^n, P^{n+1}) / n = \frac{2}{3} \ln 2.$$

Proof: We begin by defining two bounding discs for the $J\{z^2 - 1\}$. Take as a center the point 0 and fix a radius T so that the disc $D(0, T)$ compactly contains $J\{z^2 - 1\}$. Also take a radius t so that the disc $D(0, t)$ is strictly contained in the immediate basin of 0 for $J\{z^2 - 1\}$. (See Figure 6.) This gives

$$J\{z^2 - 1\} \subset D(0, T) \setminus D(0, t). \tag{10}$$

Let us calculate the scaling properties of the image of ∂P^{n+1} under the same map M_n. Again we will have that the image of ∂P^{n+1} "looks" like $J\{z^2 - 1\}$ although at a much smaller scale. We remind

the reader that M_n maps the point c_{n+1} to -1. Now we claim that the point c_{n+1} acts as the "center" of ∂P^{n+1} in the following sense:

$$M_n(\partial P^{n+1}) \subset D(-1, \frac{M_n'}{M_{n+1}'}T) \setminus D(-1, \frac{M_n'}{M_{n+1}'}t), \tag{11}$$

where M_n' represents the derivative of M_n at the point c_n. To prove the claim we note that $M_{n+1}(\partial P^{n+1}) \subset D(0, T) \setminus D(0, t)$. Pulling this image back by the univalent map $M_n \circ M_{n+1}^{-1}$ and noting that this map has increasing Koebe space for our domain proves this claim.
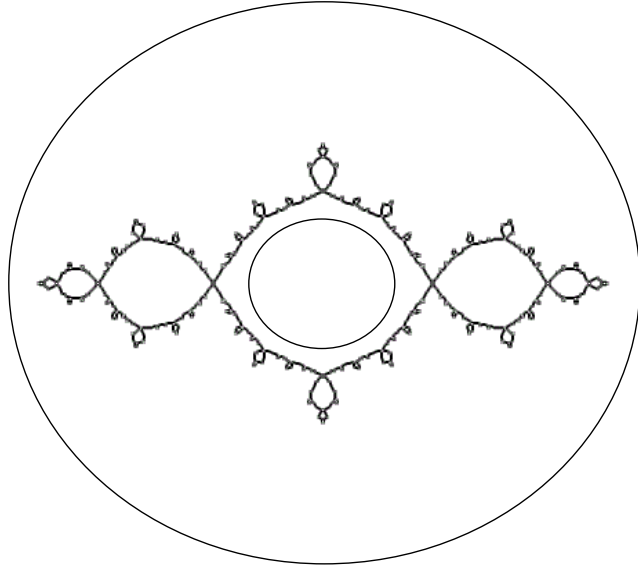

Figure 6: The centering property for the Julia set of $z^2 - 1$.

Now let us observe what is happening dynamically for all $c \in P^{n+1}$. We have that $r_{n,c}(\widetilde{V}_1^n)(c)$ is also centered around -1 by the construction of $r_{n,c}$. Hence we have a result similar to that in expression (10), although perhaps with different radii. Most importantly, however, the different radii must preserve the same centering ratio seen in expression (11), i.e., $\frac{T}{t}$.

To compare the centerings of the dynamical and parameter sets above, we focus on the Fibonacci point c_{fib}. We have that the point $M_n(c_{fib})$ is contained in the topological annulus of expression (11). But this image must also be contained in the centering annulus of $r_{n,c_{fib}}(\partial \widetilde{V}_1^n)$ in the dynamical space. Geometrically the point $M_n(c_{fib})$ is to the sets $r_{n,c_{fib}}(\partial \widetilde{V}_1^n)$ and $M_n(\partial P^{n+1})$ as the -1 point is to the Julia set of $z \to z^2 - 1$ up to exponentially small error. Hence we have the following equivalent centerings

$$r_{n,c_{fib}}(\partial \widetilde{V}_1^n)(c_{fib}) \subset D(-1, \frac{M_n'}{M_{n+1}'}T) \setminus D(-1, \frac{M_n'}{M_{n+1}'}t), \tag{12}$$

$$M_n(\partial P^{n+1}) \subset D(-1, \frac{M_n'}{M_{n+1}'}T) \setminus D(-1, \frac{M_n'}{M_{n+1}'}t). \tag{13}$$

Let us rewrite the scaling estimate of Equation (8) from Lemma 3.3,

$$\lim_{n \to \infty} \text{mod}\left(V_0^{n-1}(c_{fib}), \widetilde{V}_1^n(c_{fib})\right) \,/\, n = \frac{2}{3}\ln 2.$$

Since the modulus function is preserved under rescalings, we apply $r_{n,c_{fib}}$ to get

$$\lim_{n \to \infty} \text{mod}\left(r_{n,c_{fib}}(V_0^{n-1}(c_{fib})), r_{n,c_{fib}}(\widetilde{V}_1^n(c_{fib}))\right) \,/\, n = \frac{2}{3}\ln 2. \tag{14}$$

Expressions (12) and (13) and Equation (14) combined with Lemma 4.2 give

$$\lim_{n \to \infty} \text{mod}\left(M_n(P^n), M_n(P^{n+1})\right) \,/\, n = \frac{2}{3}\ln 2, \tag{15}$$

which proves Theorem A, part 1, and hence completes the proof of this theorem. $\odot$

6 Hairiness at the Fibonacci Parameter

Let us define the Mandelbrot dilation for the Fibonacci point given by the renormalization. We wish to dilate the Mandelbrot set, $\mathbf{M}$, about the Fibonacci parameter point by taking the approximating superstable parameter points c_n to some fixed value for each n. Of course, we have been doing a similar kind of dilation in the previous section so we will take advantage of this work and rescale in the following more well-defined manner.

Mandelbrot rescaling: Let R_n be the linear map acting on the parameter plane which takes c_{fib} to -1 and c_n to 0. Notice that this is nearly the same map as our parameter map M_n. The maps M_n have an increasing Koebe space, take c_n to 0, and asymptotically takes c_{fib} to -1.

The proof of hairiness will be a consequence of the geometry of the external rays which make up pieces of the boundary of the principal nest puzzle pieces, $V_0^n(c)$. Before proving this theorem, we first give a combinatorial description of how these rays lie in the dynamical space for the Fibonacci parameter.

We remind the reader that $\beta_{n,0}$ is on the boundary of V_0^n and is the landing point of two external rays. We label the union of these two rays of $\beta_{n,0}$ as $\gamma(\beta_{n,0})$. The curve $\gamma(\beta_{n,0})$ divides the complex plane into two regions. We label the region which does not contain the piece puzzle V_0^n as $\Gamma(\beta_{n,0})$.

We also define similar objects $\Gamma(x)$ and $\gamma(x)$ for the other Julia set points x on the boundary of V_0^n. To start, we have the symmetric point $\beta_{n,1}$ of $\beta_{n,0}$, and note $g_n(\beta_{n,1}) = g_n(\beta_{n,0})$. We can exhaust all other Julia set points on the boundary of V_0^n, denoting them as $\beta_{n,i}$ where $g_{n-i+1} \circ g_{n-i-1} \circ ... \circ g_n(\beta_{n,i}) = \beta_{n-i,0}$ for $2 \leq i \leq n$. Of course this representation is not unique in the variable i but we will not need to distinguish between these various $\beta_{n,i}$ points. For each of the $\beta_{n,i}$ points we can define $\gamma(\beta_{n,i})$ as the union of the two external rays which land there. Similarly we define the $\Gamma(\beta_{n,i})$ region as we did for $\beta_{n,0}$. In particular, $\Gamma(\beta_{n,i})$ has boundary $\gamma(\beta_{n,i})$ and does not contain V_0^n.

The combinatorial properties for the γ and Γ sets are easy to determine for the Fibonacci parameter. First we have that $|\beta_{n,0}| < |\beta_{n-1,0}|$ where the absolute values are necessary since the β's change orientation (see page 11). If the $\beta_{n,0}$ and $\beta_{n-1,0}$ have the same sign then $\Gamma(\beta_{n,0}) \supset \Gamma_{n-1}(\beta_{n-1,0})$,

otherwise we replace $\beta_{n,0}$ with its symmetric point to achieve this inclusion. By application of pull-backs of g_n it is easy to see that

$$\bigcup_i \Gamma(\beta_{n,i}) \supset \bigcup_i \Gamma(\beta_{n-1,i}). \tag{16}$$

Since this is just a combinatorial property depending on the first n Fibonacci renormalizations, this property holds as we vary our parameter c in Q^n. As a direct consequence of expression (16), we conclude that

$$J_c \cap (V_0^{n-1}(c) \setminus V_0^n(c)) \subset \bigcup_i \Gamma_n(\beta_{n,i}(c)). \tag{17}$$

By the dynamical scaling results we know that if we rescale the left side of expression (17) by $r_{n,c}$ then ∂V_0^{n-1} tends to infinity while $V_0^n(c)$ stays bounded (see Appendix, Proposition A.3). Hence for connected Julia sets the appropriate connected pieces must "squeeze through" the Γ regions in $V_0^{n-1} \setminus V_0^n$. We will be able to conclude the hairiness theorem by application of our map M_n and by the geometry of the Γ regions, i.e., the controlled "hairiness" of J_c. We show that the rescaled Γ regions, i.e., $r_{c,n}(\Gamma_n(\beta_{n,0}(c)))$ are converging to the 0-ray of $J\{z^2 - 1\}$. (Compare Figures 7 and 8 with 9.) Also we show that $r_{c,n}(\Gamma_{n+1}(\beta_{n+1,0}(c)))$ converges to the inner 0-ray of the Fatou component containing 0 for $J\{z^2 - 1\}$.
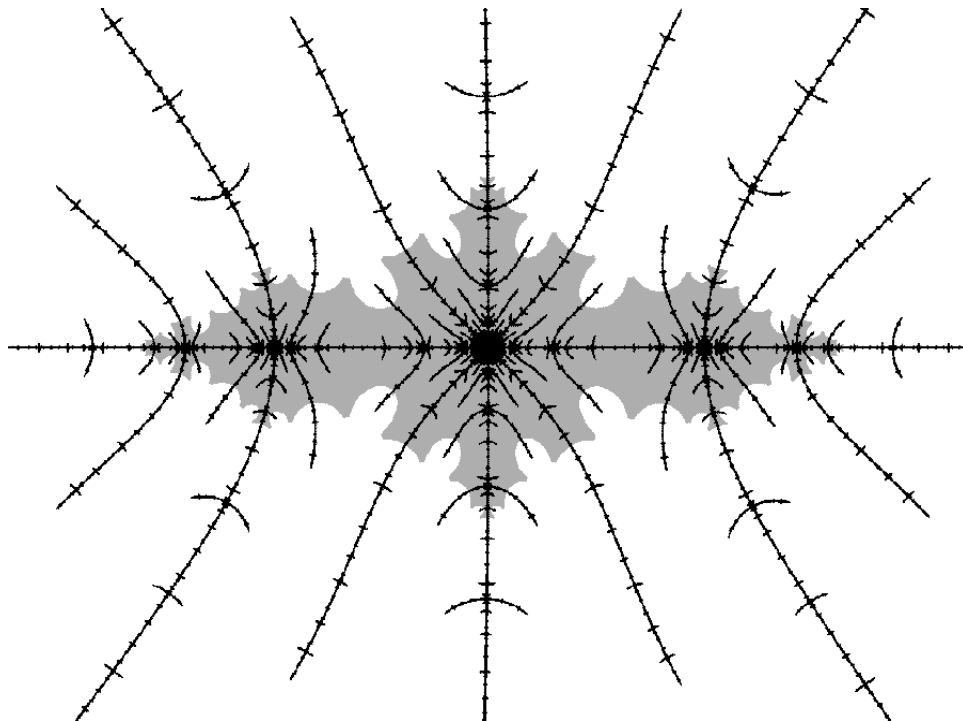

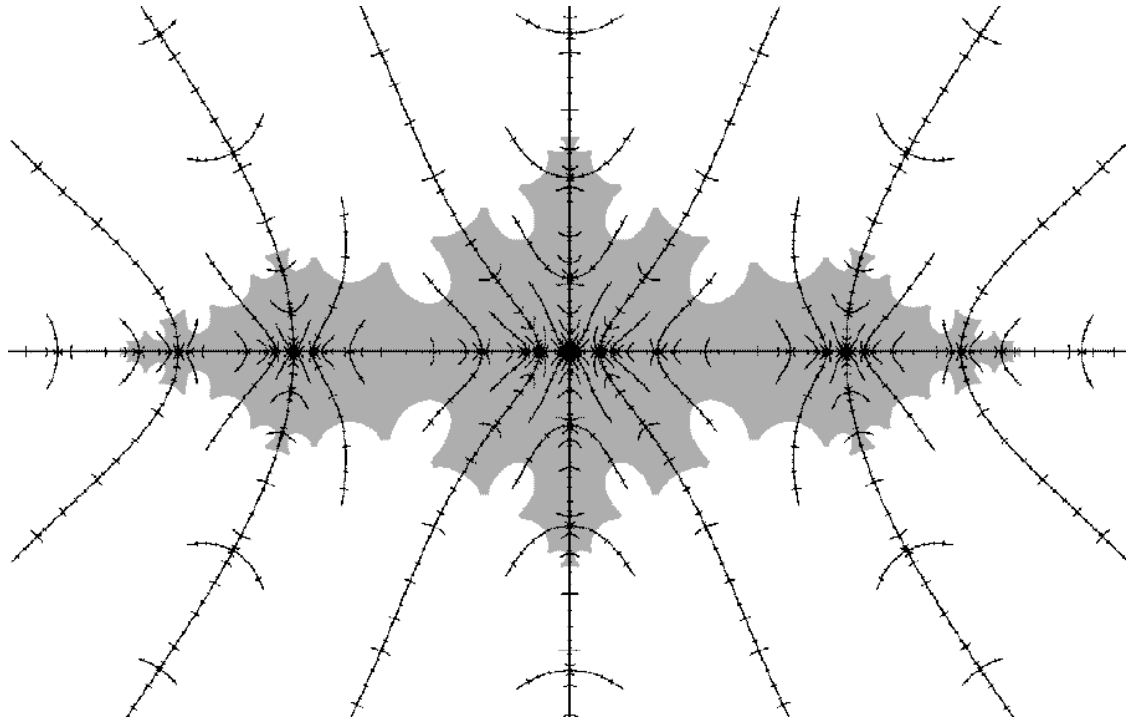Figure 7: Parapuzzle piece P^6 with Mandelbrot set.

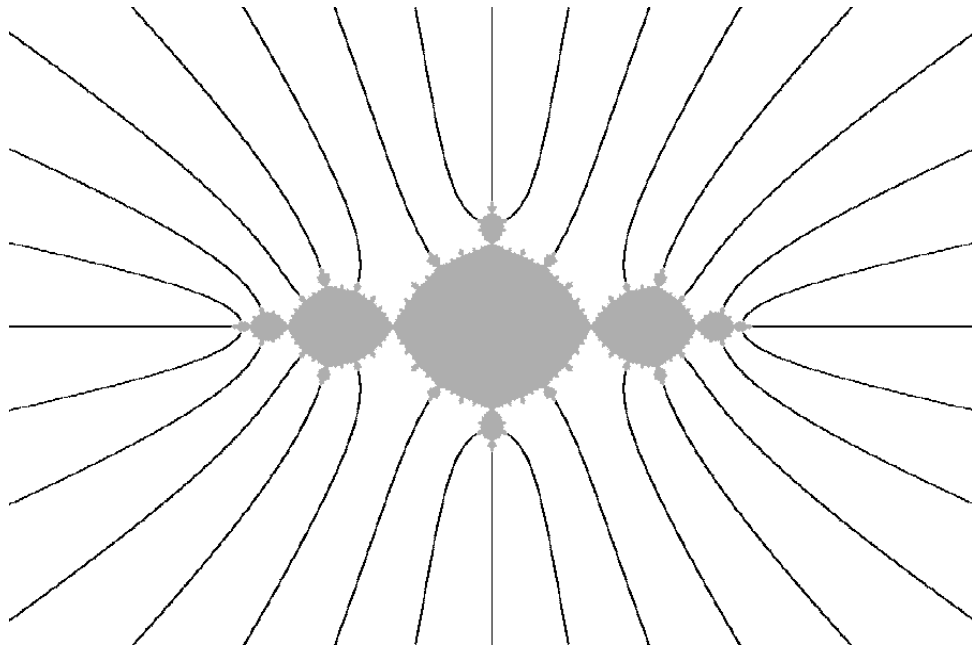Figure 8: Dynamical central puzzle piece V_0^6 for the Fibonacci Julia set.

Figure 9: The 0-ray and some of its preimages for the Julia set of $z^2 - 1$.

Lemma 6.1 *For $c \in P^n$ the linear rescaling maps $r_{n,c}$ and $r_{n,c_{fib}}$ have asymptotically the same argument, $|\arg(r_{n,c}) - \arg(r_{n,c_{fib}})| \to 0$ modulo π.*

Proof: The return maps g_n are asymptotically $z^2 - 1$ post-composed and pre-composed by a linear dilation. When our return maps have a large Koebe space we see that the rescaling argument difference (as in the Lemma) converges to a constant modulo π. For the Fibonacci parameter case we are always rescaling by a real value so the difference is 0 modulo π. Since we are scaling down to the Fibonacci parameter we get the desired result. $\odot$

Lemma 6.2 *For discs $D(0, \rho)$ in the plane, there exists an $N(\rho) > 0$ so that for all $n > N$ the curves $r_{n,c}(\Gamma(\beta_{n,0}(c)))$ converge to the 0-ray of the Julia set of $z \mapsto z^2 - 1$ in the Hausdorff metric in $D(0, \rho)$. Also, the curves $r_{n,c}(\Gamma(\beta_{n+1,0}(c)))$ converge to the inner 0-ray of the Fatou component containing 0 for the Julia set of $z \mapsto z^2 - 1$.*

Proof:

By Lemma 6.1 the rescaling maps $r_{n,c}$ converge to a real dilation. Hence there is a decreasing amount of "rotation" in the return map $g_{n,c}$. In particular, the return maps g_n are close to $z^2 - 1$ post-composed and pre-composed with a real rescaling in the C^1 topology. Let us focus on the curves $r_{n,c}(\Gamma(\beta_{n,0}(c)))$. Since we know that the pull-backs are essentially $z^2 - 1$, the curves should converge as stated in the theorem. However, there are two difficulties. First, our G_n pull-backs are not defined in all of $\mathbb{C}$ and second, $z^2 - 1$ is contracting under preimages. Hence, we check that after pulling back our curves $r_{n,c}(\Gamma(\beta_{n,0}(c)))$ by G_n that their extensions (i.e., the rescaled pull-back of the whole curve by the appropriate f iterate) have some a priori bounds.

Let us take the set $\gamma_n \cap V_0^{n-2}$ and pull-back by $g_n \circ g_{n-1}$. Taking the appropriate branches we get $(\gamma(\beta_{n+1,0}) \cup \gamma(\beta_{n+1,1}) \cup \gamma(\beta_{n+1,2})) \cap V_0^n$. In particular, the endpoints of $\gamma(\beta_{n+1,0})$ lie on the boundary of V_0^n. Hence their extension is determined by property (16) (the geometry of the rays of the previous level). In particular, we have that $\gamma(\beta_{n+1,0}) \cap (V_0^{n-1} \setminus V_0^n)$ is combinatorially between $\Gamma(\beta_{n,0})$ and $\Gamma(\beta_{n,2})$. The piece of $\gamma(\beta_{n+1,0})$ contained in V_0^n is controlled by the nearly $z^2 - 1$ pull-backs (the maps $g_{n-1} \circ g_{n-2}$ after rescaling) of again lesser level rays as constructed above. So let us assume the sets $\gamma(\beta_{j,0})$, $\gamma(\beta_{j,1})$ and $\gamma(\beta_{j,2})$, $j = \{n, n-1\}$ nicely lie in the appropriate half-planes, where nice means that $r_{c,n}(\gamma(\beta_{j,0}))$ is in the right-half plane, $r_{c,n}(\gamma(\beta_{j,1}))$ in the left-half plane, and $r_{c,n}(\gamma(\beta_{j,2}))$ in the upper-half plane. Then by the above argument we have that the collection $r_{n+1,c}(\gamma(\beta_{j,0}))$, $r_{n+1,c}(\gamma(\beta_{j,1}))$ and $r_{n+1,c}(\gamma(\beta_{j,2}))$ with $j = n + 1$ is also nice in that they lie in the appropriate half-planes. This completes the induction step.

The initial step comes from the fact that the geometry is nice in the Fibonacci case. More precisely we have that $r_{c,n}(\gamma(\beta_{n,0}))$ is contained in the right-half plane just by symmetry. If we pull-back as above we see that $r_{c,n}(\gamma(\beta_{n,0}))$ must be contained in the right-half plane. Hence we may perturb this set-up in a small parameter neighborhood to start the induction process.

Because the return maps G_n uniformly (in parameter c) approach $z^2 - 1$, we may use the a priori bounds and the coordinates from the Böttcher map of $z^2 - 1$ to conclude that the rescaled rays $r_{c,n}(\Gamma(\beta_{n,0})$ must uniformly approach the 0-ray of $z^2 - 1$ in compact sets. Finally, viewing this same pull-back argument inside of $r_{n,c}(V_0^n)$ for the curves $r_{n,c}(\Gamma(\beta_{n+1,0}(c)))$ yield convergence to the inner 0-ray and completes the lemma.

We are now in a good position to prove hairiness in an arbitrary disc $D(z, \epsilon) \subset \mathbb{C}$. We point out that if z is in $J\{z^2 - 1\}$, the theorem holds by Lemma 4.2. In this lemma we showed that the Misiurewicz points on the boundary of P^n under our rescaling map, M_n, converge to the preimages of the β fixed point of $z^2 - 1$. Note that the preimages of the β fixed point are dense in $J\{z^2 - 1\}$. Given that the map $M_n(c)$ is an exponentially small perturbation of $R_n(c)$ we must have hairiness for neighborhoods of such z and this claim is proven. In fact, the above argument shows that it suffices to show that images $M_n(\mathbf{M})$ satisfy the Theorem B.

Proof of hairiness:

Proof: We first focus on the structure of J_c for parameters c in Q^n. By Lemma 6.2, we have that $r_{c,n}(\Gamma(\beta_{n,0}(c)))$ converges to the 0-ray of $J\{z^2 - 1\}$ in bounded regions. Hence, for $c \in \mathbf{M} \cap P^n$ we must have that its Julia set in this region, i.e., $r_{c,n}(\Gamma(\beta_{n,0}(c))) \cap J_c$, also converges to the 0-ray (compare property (17)). Now the image of $M_n(\mathbf{M} \cap Q^n)$ must map into the set $\cup_c r_{c,n}(\Gamma(\beta_{n,0}(c))) \cap J_c)$. Also, this domain contains the Misiurewicz point, say c', which lands at the rescaled β point $r_{c',n}(\beta_{n-1,0})$. But $r_{c',n}(V_0^{n-1})$ is growing at an exponential rate while $r_{c,n}(\beta_{n,0})$, the "other" end of this image, converges to the β fixed point of $z^2 - 1$ for all $c \in Q^n$. Note we must have a Misiurewicz point landing near this β point as well. Because the Mandelbrot set is connected we get that a piece of the image $M_n(\mathbf{M} \cap Q^n)$ converges to the 0-ray of $J\{z^2 - 1\}$. Similarly we have convergence of $\cup_c r_{c,n}(\Gamma(\beta_{n+1,0}(c)) \cap J_c)$ to the inner 0-ray of $J\{z^2 - 1\}$. Hence pieces of $M_n(\mathbf{M} \cap Q^n)$ also have convergence to this inner 0-ray.

So given an arbitrary disc $D(z, \epsilon)$, we iterate it forward by $z^2 - 1$ until it intersects the 0-ray or inner 0-ray of the Julia set of $z \mapsto z^2 - 1$. By the above we have that this image will eventually intersect all Julia sets of $P^n \cap \mathbf{M}$. Pulling back by our almost $z \mapsto z^2 - 1$ maps shows that all Julia sets $P^n \cap \mathbf{M}$ must eventually intersect $D(z, \epsilon)$. Applying our parameter map and arguing as above yields hairiness. ⊙

A   Geometry of sets in the plane

Topological discs in the plane.

We define capacity for sets in the plane and reference the perturbation result used in this paper. We point out that there are many equivalent definitions of capacity, many of which may be found in the book of Ahlfors (chapter 2, [Ahl73]). We give one such definition. Take a topological disc, U in the plane with boundary $\partial U = \Gamma$. Fix a point $z \in U$. Let $\mathcal{R}$ be the Riemann map of the unit disc onto U with $\mathcal{R}(0) = z$.

Definition. The *capacity* of U (or Γ) with respect to the point z is

$$cap_z(U) = \ln \mathcal{R}'(0).$$

We can calculate the capacities needed for this paper. For $cap_\infty(J\{z^2 - 1\})$ we proceed as follows. Using the Böttcher map and Brolin's formula, we see that the dynamics for the attracting basin is

conjugate to the complement of the unit disc under the $z \mapsto z^2$ map. The conjugacy is in fact the Riemann mapping which has derivative precisely 1 at infinity (in the appropriate coordinate system). Hence, $cap_\infty(J\{z^2 - 1\}) = \ln 1 = 0$.

Similarly, we may calculate $cap_0(J\{z^2 - 1\})$. (Note we must only consider the connected component containing 0 for the capacity definition.) The dynamics around the critical point 0 is $z \mapsto 2z^2$ (two iterates of $z \mapsto z^2 - 1$). Again we can conjugate the immediate basin of attraction for the critical point to $z \mapsto z^2$ with domain the unit disc (again by the Böttcher map). Comparing the two maps, $z \mapsto 2z^2$ and $z \mapsto z^2$, we see that the conjugacy (Riemann map) must have derivative equal to 1/2. Hence $cap_0(J\{z^2 - 1\}) = \ln \frac{1}{2}$.

To state a perturbative result of capacity, consider all topological disc boundaries Γ in the plane with the Hausdorff metric d_H. The following result says that if we fix a point z bounded away from some Γ_∞, then exponential convergence to this curve in the Hausdorff metric yields exponential convergence in their capacities. The result is due to Schiffer and may be found in his paper [Sch38] or the book of Ahlfors [Ahl73] pages 98-99.

Theorem A.1 (Schiffer) *Given a sequence of disc boundaries Γ_i with convergence at an exponentially decreasing rate to some Γ_∞, $d_H(\Gamma_n, \Gamma_\infty) = O(p^n)$, and a point z bounded away from Γ_∞, then $cap_z(\Gamma_n) = cap_a(\Gamma_\infty) + O(p^n)$*

Topological annuli in the plane.

We take two topological open discs U_1 and U_2 in the plane such that U_2 is compactly contained in U_1. Then we may form the annulus $A = U_1 \setminus \bar{U}_2$. Every such annulus can be mapped (a *canonical map*) univalently to an annulus $\{z \mid 0 < r_1 < |z| < r_2\}$. Although an annulus can be mapped to many different such annuli, there does exist a conformal invariant, namely the ratio of the radii r_2/r_1. There are many equivalent definitions for the modulus of an annulus, one of which is given here.

Definition. The *modulus* of an annulus A, $modA$, is the conformal invariant $\log \frac{r_2}{r_1}$ resulting from a canonical map.

Theorem (Koebe: Analytic version) *Take any two topological discs U_1, U_2 with $U_2 \subset\subset U_1$, and a univalent map g with domain U_1. Then independently of the map g, there exists ' a constant K such that*

$$\frac{|g'(x)|}{|g'(y)|} < K$$

for $x, y \in U_2$. Also $K = 1 + O(\exp(-mod(U_2 \setminus U_1)))$ as $mod(U_2 \setminus U_1) \to \infty$.

Theorem (Grötzsch Inequality) *Given three strictly nested topological ' discs, $U_3 \subset U_2 \subset U_1$ in $\mathbb{C}$,*

$$mod(U_1 \setminus U_2) + mod(U_2 \setminus U_3) \leq mod(U_1 \setminus U_3).$$

Now suppose we take a sequence of $U_3(i)$, containing 0 and converging to 0, and a sequence $U_1(i)$ with boundary converging to infinity. The set U_2 will remain fixed. Also, suppose $U_3(i) \subset U_2 \subset$

$U_1(i) \subset \mathbb{C}$, then the equipotentials for the topological annuli $U_1(i) \setminus U_3(i)$ in compact regions of $\mathbb{C} \setminus 0$ converge to circles centered at 0. One consequence is the following proposition.

Proposition A.2 *Given $U_1(i)$, U_2, and $U_3(i)$, the deficit in the Grötzsch Inequality converges to* $cap_0(U_2) + cap_\infty(U_2)$.

Finally, we mention one extremal situation (see [LV73], Chapter 2 for actual estimates). Suppose we take a topological annulus $A \in \mathbb{C}$ with inner boundary Γ_1 and outer boundary Γ_2.

Proposition A.3 *If A is normalized so that the diameter of Γ_1 is equal to 1 then* $\mathrm{dist}(\Gamma_1, \Gamma_2) \to \infty$ *as* $\mathrm{mod} A \to \infty$.

References

[Ahl73]   L. Ahlfors, *Conformal Invariants, Topics in Geometric Function Theory*, McGraw-Hill, 1973.

[BH92]   B. Branner and J.H. Hubbard, *The iteration of cubic polynomials, part II*, Acta Math. **169** (1992), 229–325.

[Bro65]   H. Brolin, *Invariant Sets Under Iteration of Rational Functions*, Ark. Math. **6** (1965), 103–144.

[DH85]   A. Douady and J.H. Hubbard, *E'tude dynamique des polynomes complexes*, Publications Mathematiques d'Orsay, Universite' de Paris-Sud, 1984-1985.

[DH93]   A. Douady and J.H. Hubbard, *A proof of Thurston's topological characterization of rational functions.*, Acta Math. **171** (1993), 263–297.

[GM93]   L. Goldberg and J. Milnor, *Fixed point portraits of polynomial maps.*, Preprint 14, SUNY at Stony Brook, IMS, 1993.

[Hub93]   J.H. Hubbard, *Local connectivity of Julia sets and bifurcation loci: three theorems of J. C. Yoccoz.*, Topological Methods in Modern Mathematics, A Symposium in Honor of John Milnor's 60th Birthday, Publish or Perish, 1993.

[Lei90]   T. Lei, *Similarity between the Mandelbrot set and Julia sets*, Commun. Math. Phys. **134** (1990), 587–617.

[LM93]   M. Lyubich and J. Milnor, *The Fibonacci unimodal map.*, Journal of the AMS **6** (1993), 425–457.

[LV73]   O. Lehto and K. I. Virtanen, *Quasiconformal mappings in the plane*, Springer-Verlag, 1973.

[Lyu93a] M. Lyubich, *Geometry of Quadratic Polynomials: Moduli, Rigidity, and Local Connectivity*, Preprint 9, SUNY at Stony Brook, IMS, 1993.

[Lyu93b] M. Lyubich, *Teichmuller Space of Fibonacci maps*, Preprint 12, SUNY at Stony Brook, IMS, 1993.

[McM94]   C. McMullen, *Renormalization and 3-manifolds which fiber over the circle*, preprint, University of California at Berkley, 1994.

[Mil89]   J. Milnor, *Self-similarity and hairiness in the Mandelbrot set*, Computers in Geometry and Topolgy (Lecture Notes in Pure Appl. Math Tangora, ed.), no. 114, Beckker, 1989.

[Mil90]   J. Milnor, *Dynamics in one complex variable: Introductory lectures*, Preprint 5, SUNY at Stony Brook, IMS, 1990.

[Mil92]   J. Milnor, *Local connectivity of Julia sets: Expository lectures*, Preprint 11, SUNY at Stony Brook, IMS, 1992.

[Sch38]   M. Schiffer, *A Method of Variation within the Family of Simple Functions*, Proc. London Math. Soc. **2** (1938), 450–452.

[TV90]   F. M. Tangerman and J. J. P. Veerman, *Scalings in Circle Maps (ii).*, Commun. Math. Phys. (1990), no. 141, 279–291.